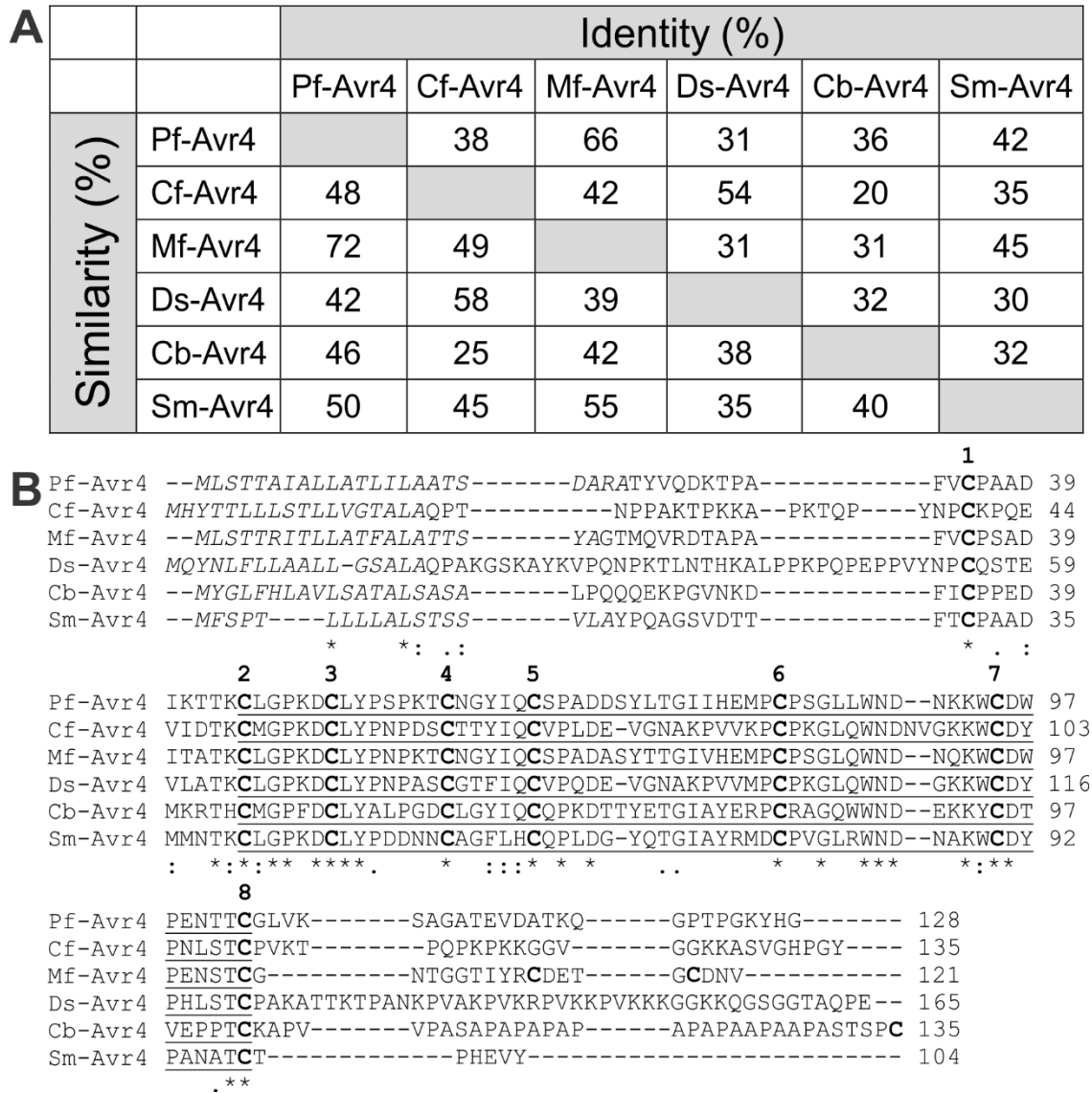


1 **SUPPLEMENTAL FIGURES**

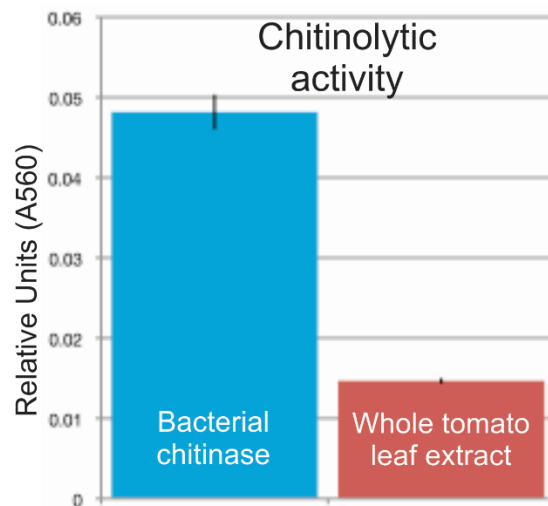


2

3 **Supplemental Figure 1.** The *Pseudocercospora fuligena* Avr4 effector protein (Pf-Avr4) is a member
4 of the Avr4 core fungal effector family.

5 **(A)** % protein identity (upper triangle) and similarity (lower triangle) scores among different members of
6 the Avr4 effector family calculated using global Needleman-Wunsch alignments. Cf-Avr4: *Cladosporium*
7 *fulvum* Avr4 (Q00363), Mf-Avr4: *Mycosphaerella fijiensis* Avr4 (XP007926047), Ds-Avr4: *Dothistroma*
8 *septosporum* Avr4 (EME41286), Cb-Avr4: *Cercospora beticola* Avr4 (ADE28519), Sm-Avr4:
9 *Sphaerulina musiva* Avr4 (EMF11067).

10 **(B)** Alignment of Avr4 homologues from different Dothideomycete species. Alignments were produced
11 using ClustalW. Conserved amino acid residues are indicated with an asterisk. Cysteine residues are
12 highlighted in bold and the eight conserved cysteine are numbered above the alignment. The putative
13 family 14 carbohydrate-binding module (CBM14: Pfam01607) is underlined and signal peptide
14 sequences are shown in italics.

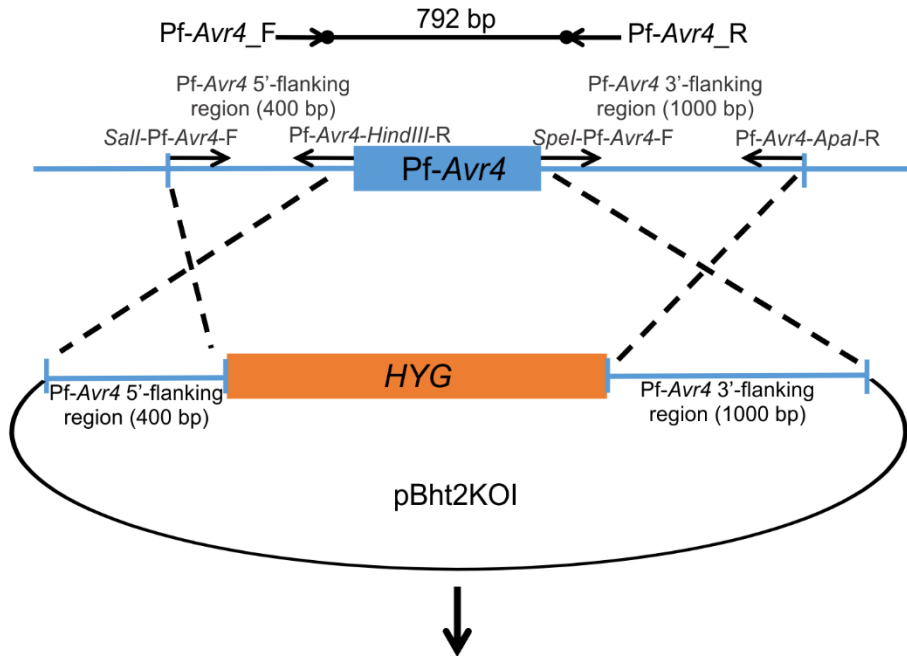


15

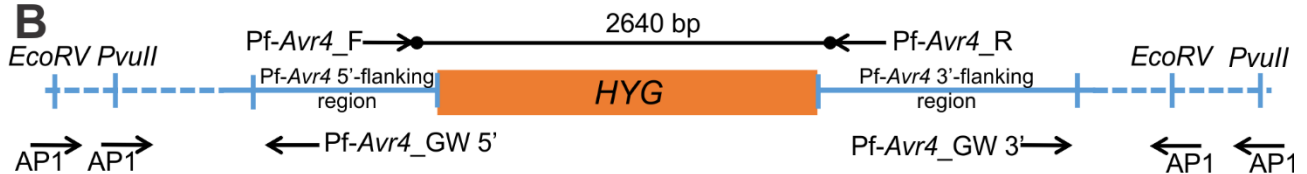
16 **Supplemental Figure 2.** Chitinolytic activity of the whole tomato leaf extract and of the bacterial
17 chitinase, as measured by treatment of chitin azure at 25°C for 7.5 hours.

18 To measure the chitinolytic activity of the whole tomato leaf extract, chitin azure was treated with either
19 bacterial chitinase or whole tomato leaf extract and incubated at 25°C for 7.5 hours. The chitin azure
20 was pelleted and an absorbance reading of A₅₆₀ was taken on the supernatant of each reaction. Activity
21 is plotted as a bar graph with standard error of the mean (SEM) indicated for each sample with a black
22 line.

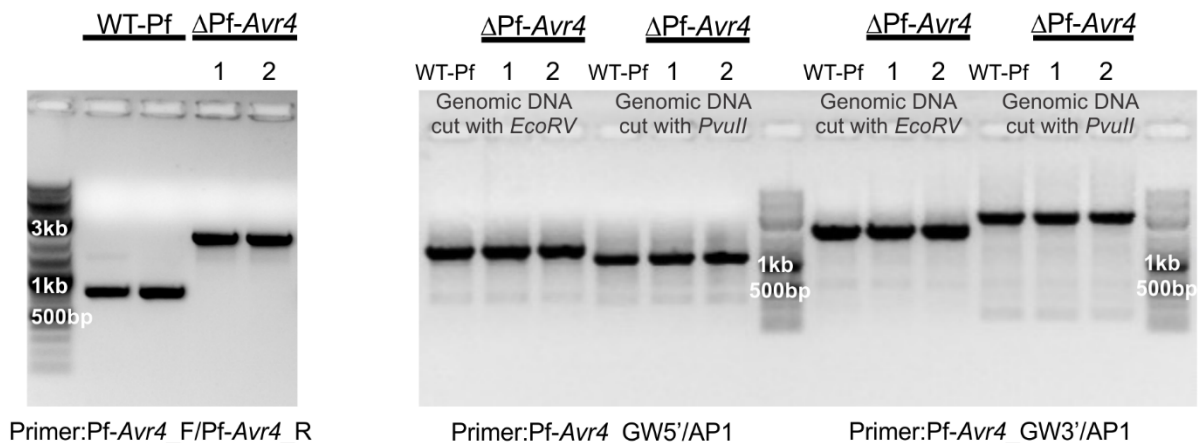
A



B



C



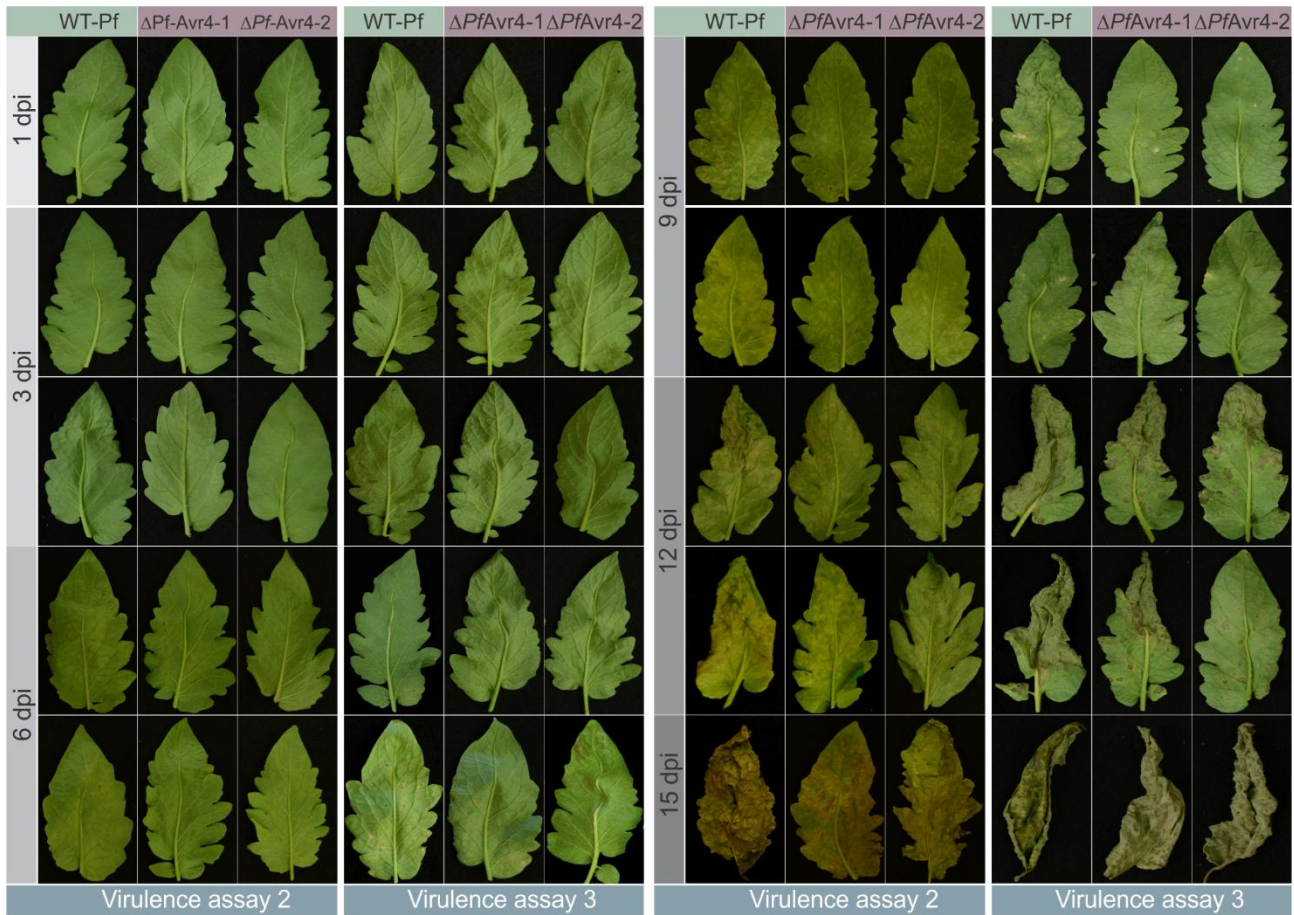
23

24 **Supplemental Figure 3.** Targeted gene replacement of Pf-Avr4 by the hygromycin-resistance cassette
 25 in the genome of *Pseudocercospora fuligena*.

26 **(A)** Schematic representation of the strategy used to generate the construct for the replacement of Pf-
 27 Avr4 by the hygromycin (*HYG*) resistance cassette. A 400 bp DNA fragment upstream of Pf-Avr4 as
 28 well as a 1 kb DNA fragment downstream of Pf-Avr4, were amplified from genomic DNA of *P. fuligena*
 29 using primer pairs *Sall*-Pf-Avr4_F/Pf-Avr4-HindIII-R (for the 400 bp fragment), and *SpeI*-Pf-Avr4-F/Pf-
 30 Avr4-ApaI-R (the 1 kb fragment). The two fragments were subsequently double-digested with *Sall* and
 31 *HindIII* (the 400 bp fragment), or *SpeI* and *ApaI* (the 1 kb fragment), and cloned into pBht2KOI binary
 32 vector at the 5'-end (the 400 bp fragment) and the 3'-end (the 400 bp fragment) of *HYG*.

33 **(B)** Schematic representation of the Pf-*Avr4* locus after replacement of Pf-*Avr4* by the *HYG*-cassette
34 (see panel **C** for further details).

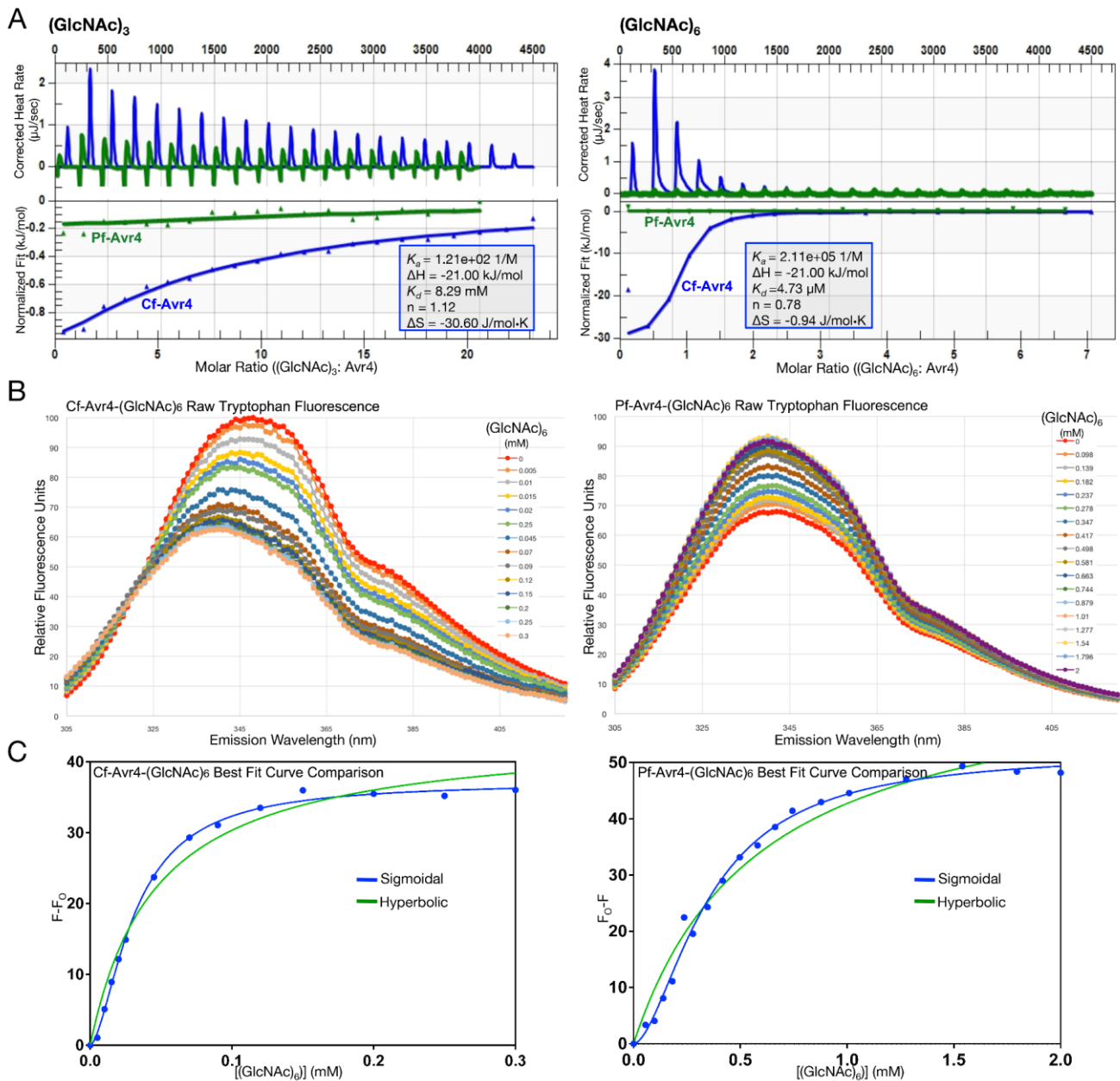
35 **(C)** The successful integration of the *HYG*-cassette in the Pf-*Avr4* locus of two Δ Pf-*Avr4* deletion
36 mutants (Δ Pf-*Avr4-1* and Δ Pf-*Avr4-2*) was verified by PCR using the primer pair Pf-*Avr4_F*/Pf-*Avr4_R*
37 (left side of panel **C**), which in case of a successful targeted Pf-*Avr4* replacement event amplifies a
38 2,640 bp fragment, whereas in the absence of a homologous recombination event in this gene locus it
39 amplifies a 792 bp fragment. The absence of any ectopic integrations of the *HYG*-cassette in the
40 background of the Δ Pf-*Avr4-1* and Δ Pf-*Avr4-2* mutant strains was verified by a genome walking
41 approach. For this purpose, genomic DNA of the wild-type *P. fuligena* strain (WT-Pf) and the two Δ Pf-
42 *Avr4* mutants was digested with restriction enzymes *EcoRV* or *PvuII* and adaptors were ligated to the
43 end of the digested DNA fragments. Subsequently, primer pairs AP1/Pf-*Avr4_GW-5'* and AP1/Pf-
44 *Avr4_GW-3'* (see panel **B**) were used for amplifying DNA fragments upstream and downstream of *HYG*-
45 cassette, respectively. Using these primers only a single PCR fragment of the same size was obtained
46 for the WT-Pf strain and the two Δ Pf-*Avr4* deletion mutants indicating a single integration event (right
47 side of panel **C**).



48

49 **Supplemental Figure 4.** Virulence of the wild-type *Pseudocercospora fuligena* strain (WT-Pf) and two
 50 Δ Pf-Avr4 deletion mutants (Δ Pf-Avr4-1 and Δ Pf-Avr4-2) on cv. LA3940.

51 Virulence assays were performed three times and shown are the results from the second and the third
 52 assay. Infected material was collected at 1, 3, 6, 9, 12, and 15 days post inoculation (dpi) from 6-9
 53 randomly selected leaves of 2-3 plants that were sprayed at the beginning of the experiment with the
 54 fungal mycelia. For time points 6, 9, 12, and 15 dpi, the pictures from two randomly selected leaves that
 55 were inoculated with the WT-Pf strain or the two Δ Pf-Avr4-1 and Δ Pf-Avr4-2 mutants are shown. For
 56 time point 1 dpi the picture from only one leaf is shown as disease symptoms are not yet visible at this
 57 time point. The results show that Δ Pf-Avr4-1 and Δ Pf-Avr4-2 show a moderate reduction in virulence on
 58 cv. LA3940.



59

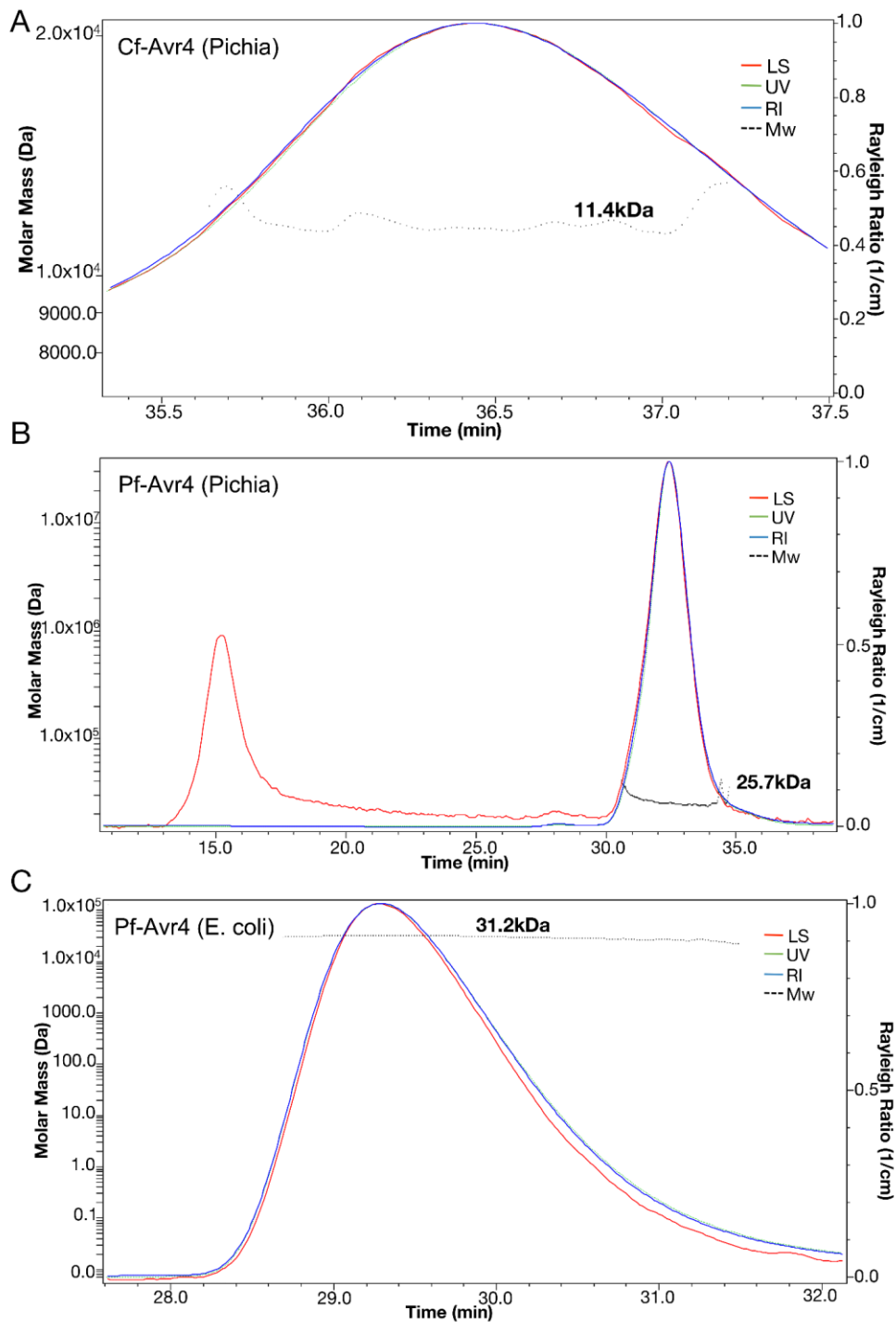
60 **Supplemental Figure 5.** The ITC and raw tryptophan fluorescence binding profiles for Cf-Avr4 and Pf-
 61 Avr4.

62 **(A)** Titration of 23 mM (GlcNAc)₃ into 0.35 mM of *Pichia*-produced Pf-Avr4 (green) or Cf-Avr4 (blue)
 63 resulted in no measurable heat change, or no quantifiable binding, for Pf-Avr4 and a binding interaction
 64 for Cf-Avr4 that was characterized by a K_d of 6.17 mM and $n=0.92$. Titration of 2 mM (GlcNAc)₆ into 0.1
 65 mM Pf-Avr4 (green) or Cf-Avr4 (blue) resulted in no measurable heat change, or no quantifiable binding
 66 for Pf-Avr4 and a binding interaction for Cf-Avr4 with a K_d of 4.7 μM and $n=0.78$. Thus, although
 67 previously reported dissociation constants for Cf-Avr4 (van den Burg et al., 2004) were readily
 68 reproducible for binding to (GlcNAc)₃ and (GlcNAc)₆, binding of Pf-Avr4 to either (GlcNAc)₃ or (GlcNAc)₆
 69 was undetectable under the testable concentrations of both Pf-Avr4 and chito-oligosaccharide, which
 70 is demonstrated by the negligible heat change detected for both the Pf-Avr4-(GlcNAc)₃ and Pf-Avr4-
 71 (GlcNAc)₆ interaction under the same conditions used for Cf-Avr4. This inability to detect binding by ITC

72 suggested that Pf-Avr4 had a lower affinity for (GlcNAc)₃ and (GlcNAc)₆ as compared to Cf-Avr4, thus
73 necessitating the use of higher working protein and chito-oligosaccharide concentrations, which was
74 not possible due to the solubility limit of Pf-Avr4 and the high viscosity of the chito-oligosaccharide at
75 required concentrations (40 mM (GlcNAc)₆).

76 **(B)** Cf-Avr4 was titrated with (GlcNAc)₆ and with each addition of (GlcNAc)₆, the sample was excited
77 with 295 nm and an emission spectrum was collected from 300-420 nm. Each curve on the graph
78 correlates to one titration point, where titration point 0 mM (shown in red) corresponds to Cf-Avr4 in the
79 absence of (GlcNAc)₆. The intrinsic tryptophan fluorescence of Cf-Avr4 decreases upon binding to
80 (GlcNAc)₆, and exhibits a blue shift in emission wavelength. Pf-Avr4 was titrated with (GlcNAc)₆
81 following the same protocol as used for Cf-Avr4. Titration point 0 mM (red) represents Pf-Avr4 in the
82 absence of (GlcNAc)₆, and upon binding to (GlcNAc)₆, the intrinsic tryptophan fluorescence of Pf-Avr4
83 increases, while the emission wavelength remains unchanged.

84 **(C)** The tryptophan fluorescence-based titration curves were best fit with a sigmoidal curve (blue)
85 defined by K_d , ΔF_{\max} , and h (hill coefficient). Shown here is the fit of (GlcNAc)₆-binding data for Cf-Avr4
86 (left) and Pf-Avr4 (right). A hyperbolic fit (K_d , ΔF_{\max}) is shown for comparison in green.



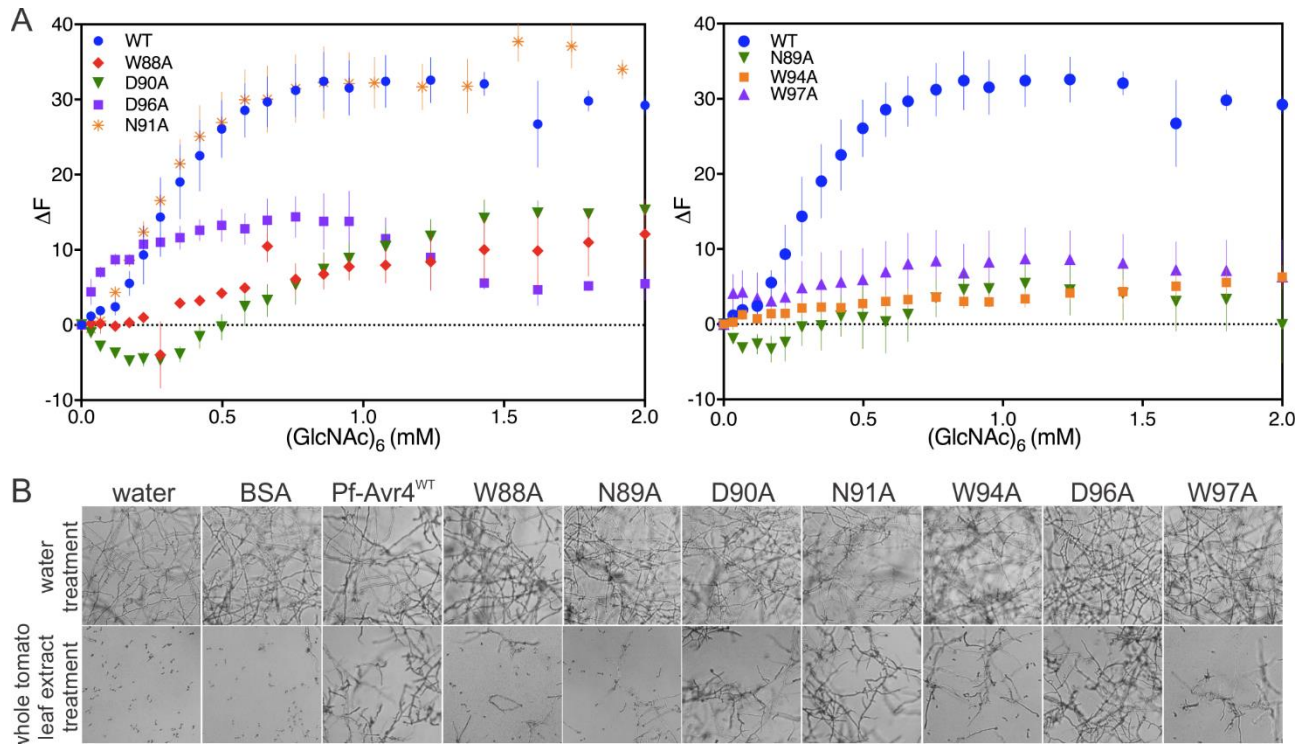
87

88 **Supplemental Figure 6.** The solution behavior of Cf-Avr4 and Pf-Avr4 as determined by SEC-MALS
 89 analysis.

90 **(A)** Cf-Avr4 produced in the methylotrophic yeast *Pichia pastoris* behaves as a monomer in solution,
 91 existing as a roughly 11.4 kDa species. The predicted molecular weight of Cf-Avr4 is 11kDa.

92 **(B)** *Pichia*-produced Pf-Avr4 exists as a dimer in solution that is approximately 25.7 kDa in size. *Pichia*-
 93 produced Pf-Avr4 has an expected molecular weight of 13 kDa.

94 **(C)** *Escherichia coli*-produced Pf-Avr4 is also a dimer in solution corresponding to roughly 31.2 kDa.
 95 The *E. coli*-produced wild-type Pf-Avr4 has an expected molecular of 17 kDa.

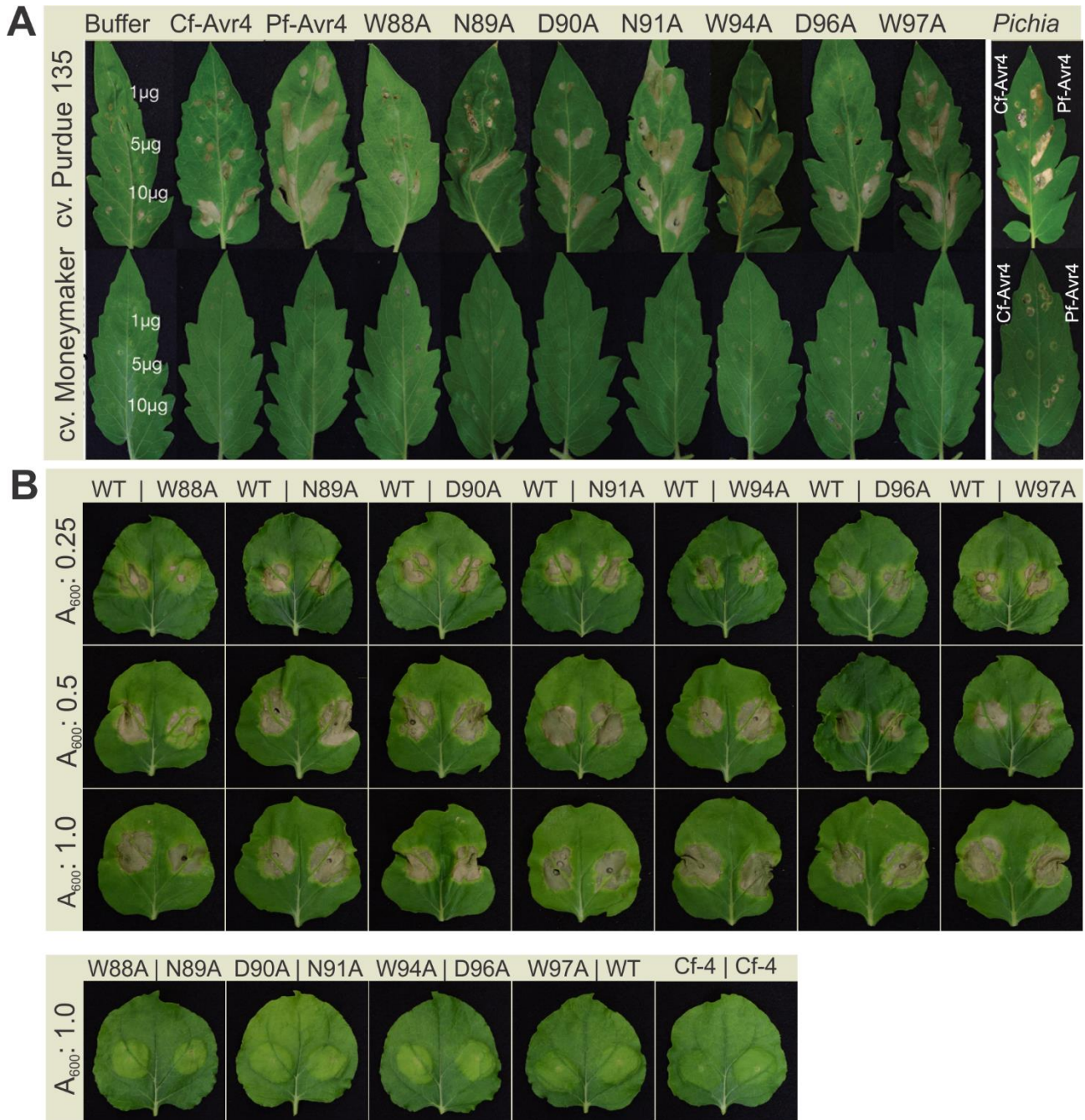


96

97 **Supplemental Figure 7.** Affinity of wild-type (WT) Pf-Avr4 and chitin-binding domain (ChtBD) mutants
 98 for (GlcNAc)₆, and their ability to provide protection against plant-derived chitinases.

99 **(A)** The individual contribution of each predicted ChtBD residue was assessed by site-directed
 100 mutagenesis to alanine and mutant affinity for (GlcNAc)₆ was measured using a tryptophan
 101 fluorescence-based binding assay. Left panel, mutations that significantly reduced Pf-Avr4's affinity for
 102 (GlcNAc)₆. Right panel, mutations that partially reduced or altered Pf-Avr4's affinity for (GlcNAc)₆.
 103 Compared to Pf-Avr4^{WT} and the other ChtBD mutants, Pf-Avr4^{D90A} exhibits a lag phase as demonstrated
 104 by the marginally negative ΔF values at titrations with (GlcNAc)₆ concentrations below 0.5 mM, following
 105 thereafter a sigmoidal binding pattern typical of the Pf-Avr4-(GlcNAc)₆ interaction. The altered
 106 fluorescence behavior of Pf-Avr4^{D90A} is likely due to a change in protein-protein association that occurs
 107 only when the protein is interacting with a true saccharide ligand (Supplemental Figure 10). ΔF
 108 represents the observed change in fluorescence upon addition of (GlcNAc)₆.

109 **(B)** The Pf-Avr4 chitin-binding domain (ChtBD) mutants offer varying degrees of protection against
 110 whole tomato leaf extracts based on their affinity for (GlcNAc)₆. *Trichoderma viride* germlings were
 111 treated with either water, BSA, Pf-Avr4^{WT}, or one of the seven ChtBD point mutants. The ability of *T.*
 112 *viride* to grow in the presence of the protein treatments is illustrated in the top row. To evaluate the
 113 ability of the ChtBD mutants to protect fungi from hydrolysis by plant-derived chitinases, the fungus was
 114 treated with whole tomato leaf extracts (bottom row).



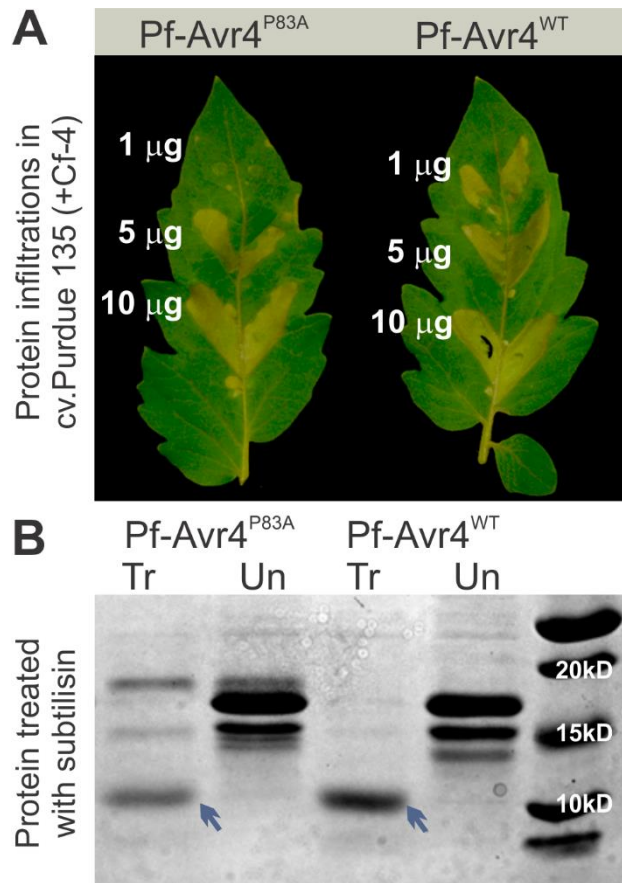
115

116 **Supplemental Figure 8.** Pf-Avr4 chitin-binding domain (ChtBD) mutants are susceptible to proteolytic
 117 cleavage under apoplastic conditions.

118 **(A)** Wild-type (WT) Pf-Avr4 and Pf-Avr4 ChtBD mutants were infiltrated into the tomato leaves of cultivar
 119 (cv.) Purdue 135 (+ Cf-4) and cv. Moneymaker (- Cf-4) at 1, 5, and 10 µg/mL concentrations, and the
 120 induction of a hypersensitive reaction (HR) was assessed at 5 days post-infiltration. The buffer alone
 121 and Cf-Avr4 were used as controls. Pf-Avr4^{WT} (*E. coli*) elicited a strong HR in cv. Purdue 135 at all
 122 concentrations tested, while Cf-Avr4 (*E. coli*) produced strong HR at 10 µg/mL and patchy HR at lower
 123 concentrations. This HR pattern for Pf-Avr4 and Cf-Avr4 was also observed when the *Pichia*-produced
 124 proteins were infiltrated in to cv. Purdue 135 and cv. Moneymaker (far right). *Pichia*-Pf-Avr4 (right) and
 125 *Pichia*-Cf-Avr4 (left) were infiltrated into the same leaf at 1, 5, and 10 µg/mL. None of the proteins

126 elicited HR in cv. MoneyMaker, suggesting that the HR response observed in cv. Purdue 135 is
127 mediated by the Cf-4 immune receptor.

128 **(B)** Pf-Avr4^{WT} and ChtBD mutants were transiently co-expressed with Cf-4 in leaves of *Nicotiana*
129 *benthamiana* using an *Agrobacterium tumefaciens* transient transformation assay (ATTA). Co-
130 infiltrations at 1:2 (A₆₀₀0.5:A₆₀₀1.0), 1:1 (A₆₀₀0.5:A₆₀₀0.5), and 1:0.5 (A₆₀₀0.5:A₆₀₀0.25) ratios of Cf-4:Pf-
131 Avr4^{WT} or one of the ChtBD mutants were tested and HR was assessed seven days post-infection.
132 Leaves were infected with Pf-Avr4^{WT}, left, and a ChtBD mutant, right. Control agroinfiltrations for the
133 individual proteins are shown in the bottom row. Of the seven ChtBD mutants, only Pf-Avr4^{W88A} elicited
134 an HR different from that of Pf-Avr4^{WT}, exhibiting a slightly weaker and patchy HR when infiltrated at
135 cell suspension densities of A₆₀₀0.25 and A₆₀₀0.5. Thus, all mutants are capable of being perceived by
136 Cf-4 when both the immune receptor and effectors are highly overexpressed using the ATTA system.
137 The differences in HR induction observed when the pure proteins are infiltrated into the leaves of Cf-4
138 tomato plants is likely due to a combination of factors, including the amount of Avr4 effector protein
139 infiltrated, the amount of Cf-4 present on the cell surface, and the type and activity level of the proteases
140 present in the tomato leaf apoplast.

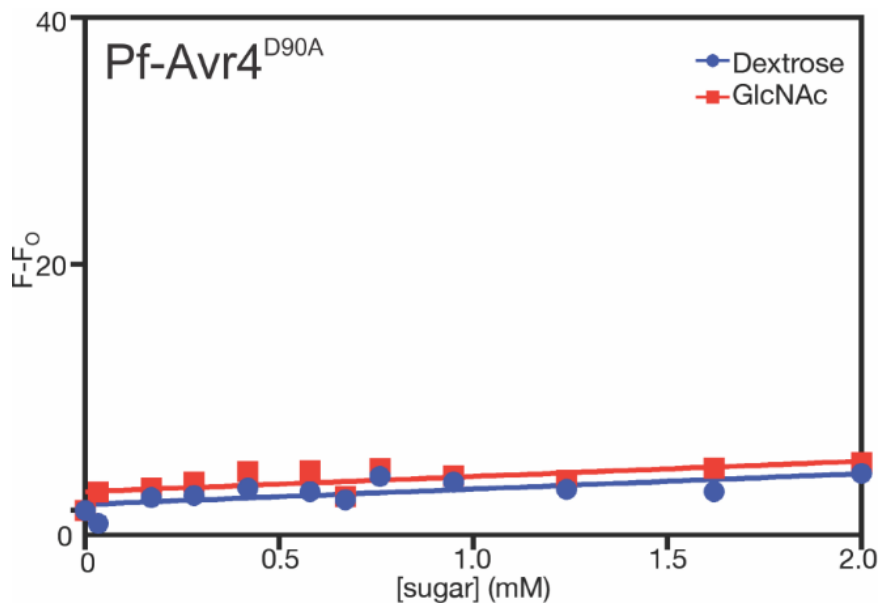


141

142 **Supplemental Figure 9.** The Pf-Avr4^{P83A} mutant is partially susceptible to proteolysis by subtilisin and
 143 is recognized by Cf-4.

144 **(A)** Wild-type (WT) Pf-Avr4 and the Pf-Avr4^{P83A} mutant were infiltrated into tomato leaves of cultivar
 145 (cv.) Purdue 135 (+ Cf-4) at 1, 5, and 10 μg/mL to determine their ability to be recognized by Cf-4 and
 146 elicit a hypersensitive response (HR). Both protein isoforms were capable of inducing HR at the
 147 concentrations of 5 and 10 μg/mL but only the Pf-Avr4^{WT} induced an HR at the concentration of 1 μg/mL.

148 **(B)** To assess whether the inability of the Pf-Avr4^{P83A} mutant to induce an HR at the concentration of 1
 149 μg/mL was due to increased proteolytic vulnerability, the Pf-Avr4^{WT} and the Pf-Avr4^{P83A} mutant were
 150 treated with subtilisin, a non-specific protease (Un: untreated protein; Tr: subtilisin-treated). Subtilisin
 151 digested both the Pf-Avr4^{WT} and the Pf-Avr4^{P83A} mutant from a 17 kD protein to a 10 kD product
 152 (indicated with a blue arrow), corresponding to the full-length, mature protein sequence. However, after
 153 treatment with subtilizing, the intensity of the band corresponding to Pf-Avr4^{P83A} mutant was almost half
 154 of the intensity of the band corresponding to the Pf-Avr4^{WT}, indicating increased proteolytic sensitivity.



155

156 **Supplemental Figure 10.** The fluorescence behavior of Pf-Avr4^{D90A} is unaffected by titration of sugars
 157 to which Pf-Avr4 does not display affinity.

158 Pf-Avr4^{D90A} was titrated with dextrose (blue) or GlcNAc (red) to a maximum of 2mM, and in the presence
 159 of either sugar, Pf-Avr4^{D90A} did not exhibit a change in fluorescence. Therefore, as sugars are known to
 160 interact with and stabilize protein structures, the unique binding pattern observed with titration of Pf-
 161 Avr4^{D90A} with (GlcNAc) (Supplemental Figure 7A) is likely due to a change in Pf-Avr4^{D90A} tryptophan
 162 fluorescence that occurs in the presence of a true binding ligand.

163 **SUPPLEMENTAL REFERENCES**

164 **van den Burg, H.A., Spronk, C.A.E.M., Boeren, S., Kennedy, M.A., Vissers, J.P.C., Vuister, G.W.,**
 165 **de Wit, P.J.G.M., and Vervoort, J.** (2004). Binding of the AVR4 elicitor of *Cladosporium fulvum*
 166 to chitotriose units is facilitated by positive allosteric protein-protein interactions - The chitin-
 167 binding site of AVR4 represents a novel binding site on the folding scaffold shared between the
 168 invertebrate and the plant chitin-binding domain. J. Biol. Chem. **279**, 16786-16796.

169

SUPPLEMENTAL TABLES

170

Supplemental Table 1. Primers used for *Pf-Avr4* gene expression analysis and targeted gene replacement.

171

Primer name	Primer sequence
<i>Pf-Avr4_F</i>	5'-CAATGCCAAGAGTCCAAACA-3'
<i>Pf-Avr4_R</i>	5'-AGAAGACTGGAGGAACTTGG-3'
<i>Pf-Avr4_qPCR-F</i>	5'-CGCCAGCAGATGACTCCTA-3'
<i>Pf-Avr4_qPCR-R</i>	5'-CAGGCCAATCACACCACTTCT-3'
<i>Pf-Actin-F</i>	5'-TTTGCTACGTTGCCCTTGAC-3'
<i>Pf-Actin-R</i>	5'-GCTCGTTGCCAATAGTGATG-3'
<i>Sall-Pf-Avr4-F</i>	5'-GTCGACTGCGATGTGTCTTAAAAA-3'
<i>Pf-Avr4-HindIII-R</i>	5'-AAGCTTATAAAGCGGCTCCTGAACTGT-3'
<i>SpeI-Pf-Avr4-F</i>	5'-ACTAGTAACGGCGTCATTCCAACACTG-3'
<i>Pf-Avr4-ApaI-R</i>	5'-GGGCCCTTCAACTCGACCGATTTCGC-3'
AP1	5'-GTAATACGACTCACTATAGGG-3'
<i>Pf-Avr4_GW-5'</i>	5'-AAAACCGACAATGTGGACAGTTCAGG-3'
AP1/ <i>Pf-Avr4_GW-3'</i>	5'-CTAGCAGTTCTGGCAATTGCGTATCTGG-3'
<i>RPL2-F</i>	5'-ATGGGTCGTGTGATCAGAGCA-3'
<i>RPL2-R</i>	5'-ACAAGTGAATGGCTTAAGCCT-3'

172